The Cu-Ir (Copper-Iridium) System

63.546 192.22

By D.J. Chakrabarti* and D.E. Laughlin
Carnegie Mellon University

The broad features of the Cu-Ir equilibrium diagram are reasonably well established. This is so despite the fact that the system has been studied only in part. A broad, gently sloping liquidus stretches across the diagram; near the Cu-end, the liquid undergoes a peritectic transformation. Limited terminal solid solubility fields occur with both (Cu) and (Ir), and the (Ir) solidus exhibits retrograde behavior above the peritectic temperature. There is no experimental report of the occurrence of any intermediate or metastable phases, nor are there reports on the thermodynamic properties of the alloys.

Equilibrium Diagram

The equilibrium phases in the Cu-Ir system are: (1) the liquid, L, miscible in all proportions and stable down to the melting point of Cu at 1084.87 °C [Melt]; (2) the fcc (Cu) solid solution with a maxium solubility of ~8 at.% Ir at 1138 ± 5 °C [69Rau]; and (3) the fcc (Ir) solid solution with a maximum solubility of 6.3 at.% Cu at 1850 °C.

[69Rau] completed the major experimental work on the Cu-Ir system. The Cu-Ir equilibrium diagram shown in Fig. 1 is derived from [69Rau] for temperatures below 1200 °C. The higher temperature portion of the diagram (above 1138 °C) is estimated in this evaluation from calculations based on thermodynamic modeling of the experimental phase diagram (see "Thermodynamics"). The only other experimental study of this system was reported in [32Lin], whose electrical conductivity measurements indicated that at least 0.48 at.% Ir was soluble in (Cu) at 700 to 850 °C.

[69Rau] used differential thermal analysis (DTA) to determine both the solidus and the liquidus between 2 and 10 at.% Ir and the solidus at 50 at.% Ir. The solvus for (Cu) and the solvus and solidus for (Ir) were determined by X-ray and optical microscopy. The alloys were prepared from electrolytic Cu and (unspecified) high-purity Ir in the arc furnace. They were heat treated in a vacuum at temperatures between 700 and 1090 °C for the solid and up to 1600 °C for the solid-plus-liquid two-phase alloys.

In the absence of any experimental results at higher temperatures, the tentative diagram suggested by [69Rau] indicates complete miscibility between Cu and Ir in the liquid state, which is in qualitative agreement with the results of the thermodynamic analysis presented in this evaluation. In the solid condition, however, Cu and Ir have restricted mutual solubility, which is quite unlike the behavior of Cu with Rh, in the same group as Ir, or with the neighboring Pt and Pd, all of which exhibit complete miscibility in the solid.

*Present address: Alcoa Technical Center, Alcoa Center, PA 15069.

Fig. 1 Assessed Cu-Ir Phase Diagram

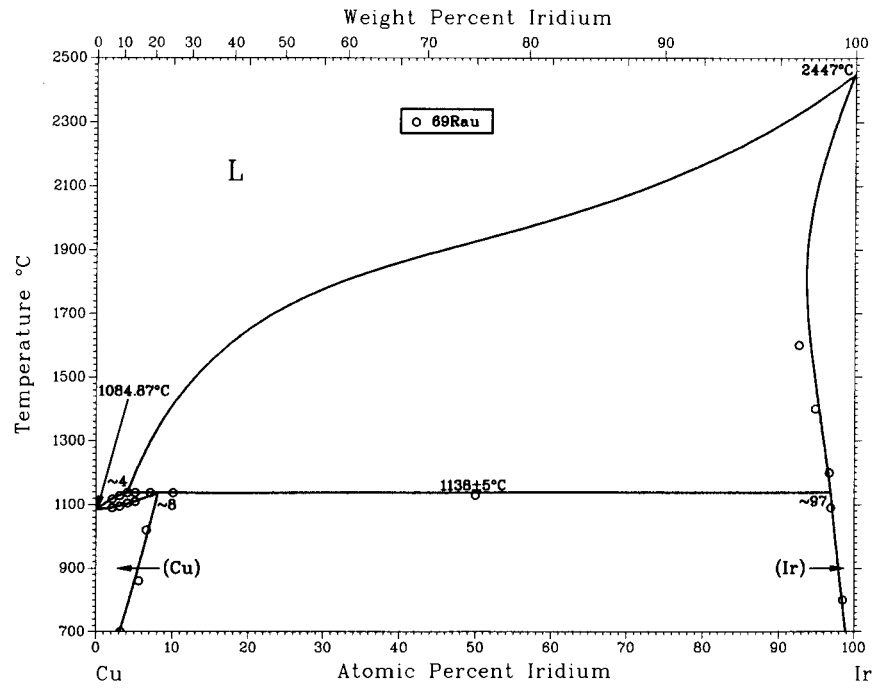

D.J. Chakrabarti and D.E. Laughlin, 1987.

Table 1 Liquidus, Solidus, and Solvus in the Cu-Ir System

Temperature, °C	Composition, at.% Ir				Reference
	Liquidus	Solidus	Solvus (Cu)	Solvus (Ir)	
2447	100	100	...	...	[Melt]
1084.87	0	0	...	...	
1600	...	92.7	...	...	[69Rau]
1400	...	94.9	...	...	
1200	...	96.8	...	...	
1090	...	...	...	97.0	
1020	...	...	6.5	...	
860	...	...	5.5	...	
800	...	...	...	98.6	
700	...	...	3.1	...	
2400	97.2	99.3	...	...	(a)
2200	82.9	96.3	...	...	
2000	61.0	94.3	...	...	
1800	32.2	93.7	...	...	
1600	17.3	94.3	...	...	
1400	9.5	95.4	...	...	
1200	5.0	96.6	...	...	
1138	4.0	97.0	...	...	
1138	...	...	8.0	97.0	(b)
1100	...	...	7.3	97.3	
900	...	...	4.1	98.7	
800	...	...	2.8	99.2	
700	...	...	1.9	99.5	
500	...	...	0.6	99.9	

(a) Calculated from Eq 2 and 3. (b) Calculated from Eq 3.

Table 2 Cu-Ir Crystal Structure Data

Phase	Composition, at.% Ir	Pearson symbol	Space group	Strukturbericht designation	Prototype
(Cu)	0 to ~8	*cF4*	*Fm3m*	*A1*	Cu
(Ir)	~93.7 to 100	*cF4*	*Fm3m*	*A1*	Cu

Thermodynamically, the Cu-Ir system is not very different from the Cu-Rh system, in that clustering effect predominates in both systems (unlike Cu-Pt and Cu-Pd alloys). The critical point of the (metastable) miscibility gap between the two fcc terminal solid solution phases in the Cu-Ir system extends above the solidus (see Fig. 2), whereas it lies below the solidus in the Cu-Rh system [82Cha]. Thus the intersection of the miscibility gap with the solidus gives rise to a peritectic-type diagram in the Cu-Ir system. The peritectic invariant temperature as obtained by DTA measurements is 1138 ± 5 °C, and the corresponding reported compositions of the liquid, (Cu), and (Ir) phases are ~4, ~8, and ~97 at.% Ir, respectively [69Rau].

The liquidus, as accepted in this evaluation and shown in Fig. 1, is based on the DTA measurements of [69Rau] for up to 4 at.% Ir, above which it is estimated from thermodynamic calculations. The melting point values of Cu and Ir at 1084.87 and 2447 °C, respectively, were obtained from [Melt].

The solidus for up to ~8 at.% Ir was determined by thermal analysis. The Cu-rich solvus was determined by the X-ray lattice parameter method; the results are shown in Table 1. The solvus and the solidus boundaries for the (Ir) phase were also obtained from lattice parameter measurements, but with the assumption (in the absence of actual data) that Vegard's law was valid for these alloys [69Rau]. If this assumption is not valid, the resultant solidus boundary will vary from the actual one, especially at compositions further away from pure Ir. Therefore, the solidus boundary for the (Ir) phase, as argued below, is accepted tentatively from the thermodynamic analysis results. Both the experimental results of [69Rau] and the present calculations indicate a retrograde solidus for the (Ir) phase. This is consistent with the very large melting point difference between Ir and Cu, and the restricted solubility field in the (Ir) phase [66Pri]. There is no report of any intermediate phase in the Cu-Ir system. Thermodynamic analysis indicates instead a clustering tendency at lower temperatures.

Metastable Phases

There is no report of any metastable phases in the Cu-Ir system. The metastable miscibility gap of the liquid as calculated from the thermodynamic analysis of the equilibrium diagram data is shown in Fig. 2.

Crystal Structures and Lattice Parameters

Cu and Ir both have fcc crystal structures (see Table 2); lattice parameters for (Cu) and (Ir) are presented in Table 3. The lattice parameter of Cu increases with the addition

Fig. 2 Cu-Ir Experimental vs Calculated Phase Diagram

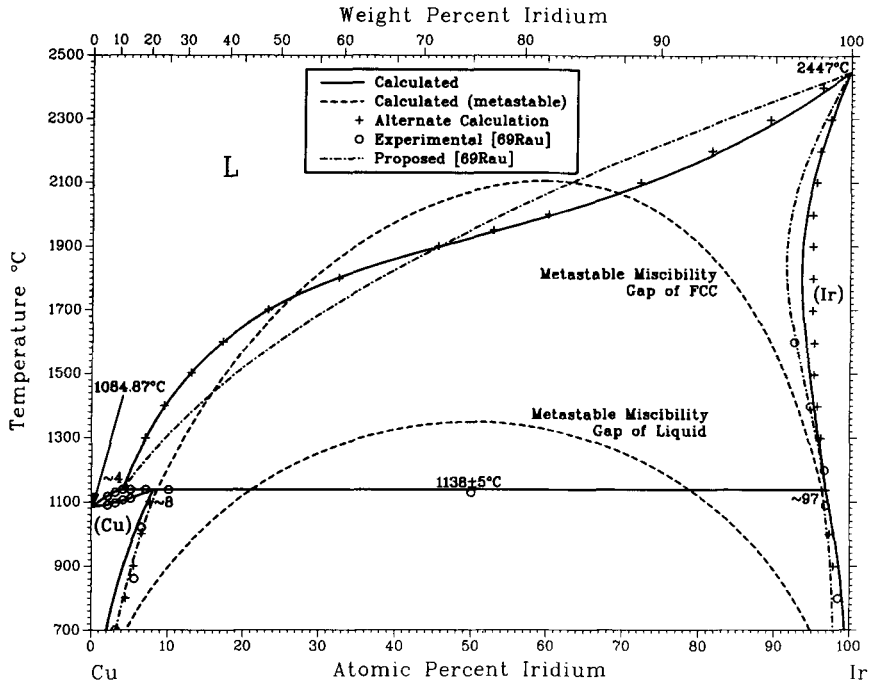

-----and--- = from Eq 2 and 3; + + + = from Eq 4 to 6.

D.J. Chakrabarti and D.E. Laughlin, 1987.

Table 3 Cu-Ir Lattice Parameter Data

Lattice parameter, nm	Comment	Reference
(Cu)		
0.36147	100% Cu at 18 °C	[Landolt]
0.3621	2 at.% Ir at 860 °C	[69Rau]
0.3623	3 at.% Ir at 860 °C	[69Rau]
0.3625	4 at.% Ir at 860 °C	[69Rau]
0.3629	5 at.% Ir at 860 °C	[69Rau]
(Ir)		
0.38390	"specpure" Ir at 30 °C	[68Sin]
0.3836	40 at.% Ir at 800 °C	[69Rau]
0.3832	60 at.% Ir at 1200 °C	[69Rau]
0.3828	60 at.% Ir at 1400 °C	[69Rau]
0.3823	60 at.% Ir at 1600 °C	[69Rau]

of Ir following a positive deviation from Vegard's law [69Rau]. The fcc crystal structure of Ir has been observed to persist down to 4.2 K [68Sch]. The lattice parameter values for the (Ir) phase shown in Table 3 are derived from the two-phase alloys at thermal equilibrium at the respective temperatures indicated and correspond to the saturation compositions of the (Ir) phase at those temperatures.

Thermodynamics

No thermodynamic measurements have been reported for the Cu-Ir alloys. [79Les] calculated several Cu-Ir equilibrium diagrams based on the subregular solution model, using several combinations of the interaction parameters for liquid and fcc phases that were determined from the experimental diagram of [69Rau]. Their diagrams show large deviations either in the liquidus or in the peritectic temperature from the diagram given by [69Rau].

Because no experimental thermodynamic data exist, the equilibrium diagram of [69Rau] has been utilized in this evaluation as a source of thermodynamic information for the different phases. The equilibrium compositions between the liquid, (Cu), and (Ir) phases, which are fairly well established between 700 °C and the peritectic temperature at 1138 °C, were used to determine thermodynamic expressions for these phases. The resulting thermodynamic parameters could be used to reproduce the (Cu) and (Ir) phase boundaries as a check for self consistency, and also to calculate the liquidus not determined experimentally.

Because the (Ir) and (Cu) phases have the same crystal structure (fcc), their interaction parameters are assumed to be identical. The phase diagram data at the peritectic temperature, 1138 °C, where the liquid having 4 at.% Ir coexists with (Cu) of 8 at.% Ir and (Ir) of 97 at.% Ir, were utilized to derive expressions for the integral molar excess Gibbs energy G^{ex} of the liquid and the fcc phase. The G^{ex} for both phases is expressed in the following form:

$$G^{ex} = X(1 - X)\sum_{i=1}^{N}(a_i^H X^{i-1} - Tb_i^S X^{i-1}) \qquad \text{(Eq 1)}$$

where a_i^H and b_i^S are, respectively, the coefficients of the enthalpy and entropy of mixing functions of the respective phases, and X is the mole fraction of Ir. The coefficients are assumed to be independent of temperature. The number of a^H and b^S terms derived from the standard multiple least-squares regression analysis of the phase coexistence data was kept to a minimum, as a compromise between

the reproducibility of the calculated diagram and the simplicity of the model [86Cha].

In the present instance, approximations of the fcc phases by a subregular solution and the liquid by a regular solution were found to be adequate for reproducing the phase diagram above the peritectic temperature. The corresponding expressions of G^{ex} for the liquid and the fcc phases are shown below in Eq 2 and 3, respectively.

$$G^{ex}(L) = X(1 - X)\,(26\,990)\ (J/mol) \quad \text{(Eq 2)}$$

$$G^{ex}(fcc) = X(1 - X)\,(32\,980 + 10\,360\,X)\ (J/mol) \quad \text{(Eq 3)}$$

According to Eq (2), the maximum value of $\Delta H(L)$ is 6.75 kJ/mol at $X = 0.50$. The corresponding integral molar Gibbs energy $G(L)$ (based on pure liquid Cu and pure liquid Ir as standard states), estimated at 1000 °C is −0.59 kJ/mol. These same values for the fcc phase are 9.58 kJ/mol at $X = 0.53$ for $\Delta H(fcc)$, and 2.27 kJ/mol at 1000 °C for $\Delta G(fcc)$.

Using Eq 2 and 3, the liquidus and the (Ir) phase boundaries were calculated as shown by a solid line in Fig. 2. In the absence of any experimental results for the liquid, the calculated diagram was compared for reproducibility against the solidus for the (Ir) phase, part of which (up to 1600 °C) is known from the work of [69Rau]. The calculated solidus shows satisfactory agreement with the latter. Incorporation of an additional entropy term in the $G^{ex}(fcc)$ expression does not improve further the reproducibility of the phase diagram. On the other hand, if the $G^{ex}(fcc)$ is represented by a combination of one enthalpy and an entropy term, or if the liquid was allowed to assume nonregularity, the resultant calculated solidus differs considerably from the diagram of [69Rau]. The resultant liquidus boundaries also exhibit large deviations from those shown in Fig. 1 or in [69Rau]. Thus, Eq 2 and 3 are considered most appropriate and are accepted in this evaluation to represent the thermodynamic properties of the liquid and the fcc phase, respectively.

The validity of the calculated liquidus was further assessed through another analysis. It was assumed that, although the (Cu) and (Ir) phases have the same crystal structure, differences in the atomic properties can introduce large local variations in the Gibbs energy curves in the narrow terminal solid solution ranges, where the G^{ex} may be approximated by two independent expressions for these isomorphous phases. Under such circumstances, the equilibrium compositions of the (Cu) and (Ir) phases at several temperatures from 700 and 1138 °C, as obtained from the solvus boundaries given by [69Rau], can be utilized to derive the expresssion for G^{ex} for (Cu) and (Ir), as in Eq 4 and 5 below:

$$G^{ex}(Cu) = X(1 - X)\,(26\,450 + 49\,130\,X)\ (J/mol) \quad \text{(Eq 4)}$$

$$G^{ex}(Ir) = X(1 - X)\,(181\,600 - 147\,400\,X)\ (J/mol) \quad \text{(Eq 5)}$$

As expected, the calculated solvus boundaries based on Eq 4 and 5 show better agreement with the experimental boundaries than do calculated boundaries based on Eq 3, which uses a single expression for the G^{ex} for both (Cu) and (Ir) (see Fig. 2). Equations 4 and 5 and the three-phase equilibria data at 1138 °C were utilized to derive the G^{ex} for the liquid for a regular solution model as in Eq 6 below.

$$G^{ex}(L) = X(1 - X)\,(26\,850)\ (J/mol) \quad \text{(Eq 6)}$$

Table 4 Thermodynamic Parameters in the Cu-Ir System

Lattice stability parameter (a)

$\Delta G_{Cu}^{s\to L} = 13\,054 - 9.613\,T$
$\Delta G_{Ir}^{s\to L} = 26\,137 - 9.609\,T$

Integral molar excess Gibbs energy (b)

$G^{ex}(L) = X(1 - X)(26\,990)$
$G^{ex}(fcc) = X(1 - X)(32\,980 + 10\,360X)$

Note: X = mole fraction of Ir; all units are in J/mol; standard states are pure liquid Cu and pure liquid Ir.
(a) [Hultgren, E]. **(b)** This work.

The liquidus and the (Ir) solidus calculated from Eq 5 and 6 are shown by plus (+) marks at selected temperatures in Fig. 2. The liquidus is identical with that calculated from Eq 2 and 3, and the solidus indicates slightly lower solubility. The above calculations indicate good internal consistency in the liquidus derived from the thermodynamic analysis of the experimental phase diagram.

The thermodynamic consistency between the calculated liquidus and solidus derived from Eq 2 and 3 was further checked at the Ir-rich end with the van't Hoff's relationship. Specifically, the distribution coefficient, K, of Cu in the liquid and (Ir) phases at very dilute ranges was determined from the initial slopes of the liquidus and the solidus, and was compared with the theoretical value of K as given by the following expression [68Gor]:

$$X_{Cu}^{(Ir)}/X_{Cu}^{L} = 1 + [\Delta H_{Ir}^{s\to L}/\,R(T_{Ir}^{m})^2]\,(\Delta T\,/\,X_{rCu}^{L})$$

In this equation, $\Delta T/X_{Cu}^{L}$ is the initial slope of the liquidus, T_{Ir}^{m} is the melting point of Ir (2447 °C), and $\Delta H_{Ir}^{s\to L}$ is the enthalpy of fusion of Ir (26 137 J/mol [Hultgren, E]). The value of K as obtained from Fig. 1 is approximately 0.28 ± 0.01 and compares very well with the theoretical value of 0.29 ± 0.02 (obtained from Eq 7 using the initial slope of the liquidus −1667 °C/X_{Cu}^{L} from Fig. 1). The corresponding values of K from the suggested curves of [69Rau] are, respectively, ~0.25 and 0.62 ± 0.03, which indicate a much greater discrepancy. Thus, the liquidus and the solidus for (Ir) as obtained from Eq 2 and 3 are considered to be consistent thermodynamically, as well as with the limited available experimental results, and are accepted in this evaluation. The solvus, and the solidus and liquidus boundaries below the peritectic temperature, are accepted from the experimental results of [69Rau], as shown in Fig. 1. The accepted thermodynamic parameters for the different phases are presented in Table 4.

Figure 1 shows slight discrepancy between the calculated and the experimental solidus for the (Ir) phase above 1300 °C. However, the experimental results, especially at higher solute ranges, may not be very reliable, if the (Ir) phase deviates from Vegard's law. In the (Cu) phase, the authors observed a positive deviation from Vegard's law. A negative deviation from Vegard's law in (Ir) is required to account for the decreased solubility indicated by the calculated solidus.

The calculated liquidus in Fig. 1 shows an inflection point, which indicates the likelihood that the liquid develops a metastable miscibility gap at lower temperatures. The metastable gap of the liquid was calculated and is shown in Fig. 2, with the critical temperature at ~1350 °C. The

symmetric shape of the gap is a consequence of the liquid being approximated as a regular solution. Figure 2 also shows the metastable miscibility gap of the fcc phase calculated from Eq 3.

Suggestion for Future Experimental Work

For the sake of completeness of the assessed phase diagram and for comparison with the calculated liquidus, the liquidus in the Cu-Ir system must be determined experimentally.

Cited References

32Lin: J.O. Linde, "Electrical Properties of Dilute Alloys," *Ann. Phys., 15* (226), 219-248 (1932) in German. (Equi Diagram; Experimental)

66Pri: A. Prince, *Alloy Phase Equilibria*, Elsevier, Amsterdam, 78 (1966). (Equi Diagram, Thermo; Review)

68Gor: P. Gordon, *Principles of Phase Diagrams in Materials Systems*, McGraw-Hill, New York, 140 (1968). (Equi Diagram, Thermo; Review)

68Sch: H.F Schaake, "Thermal Expansion of Ir from 4.2 to 300 K," *J. Less-Common Met., 15*, 103-105 (1968). (Crys Structure; Experimental)

68Sin: H.P. Singh, "Determination of Thermal Expansion of Ge, Rh, and Ir by X-Rays," *Acta Crystallogr. A, 24*, 469-471 (1968). (Crys Structure; Experimental)

***69Rau:** E. Raub and E. Roeschel, "Copper-Iridium Alloys," *Z. Metallkd., 60*, 142-144 (1969) in German. (Equi Diagram, Crys Structure; Experimental; #)

79Les: A.G. Lesnik, V.V. Nemoshkalenko, and A.A. Ovcharenko, "Computer-Aided Calculation of Constitution Diagrams of Some Binary Alloys in the Subregular Solution Approximation," *Akad. Nauk Ukr. SSR., Metallofiz, 75*, 20-31 (1979) in Russian. (Equi Diagram, Thermo; Theory; #)

82Cha: D.J. Chakrabarti and D.E. Laughlin, "The Cu-Rh System," *Bull. Alloy Phase Diagrams., 2*(4), 460-462 (1982). (Equi Diagram, Crys Structure; Compilation; #)

86Cha: D.J. Chakrabarti and D.E. Laughlin, "Critical Evaluation and Thermodynamic Modeling of Selected Copper Based Binary Alloys," in *Noble Metal Alloys*, T.B. Massalski, W.B. Pearson, L.H. Bennett, and Y.A. Chang, Ed., TMS-AIME, Warrendale, PA, 247-264 (1986). (Thermo; Theory)

* Indicates key paper.
\# Indicates presence of a phase diagram.

Cu-Ir evaluation contributed by **D.J. Chakrabarti** and **D.E. Laughlin,** Department of Metallurgical Engineering and Materials Science, Carnegie-Mellon University, Pittsburgh, PA 15213, USA. Work was supported by the International Copper Research Association, Inc., (INCRA) and the Department of Energy through the Joint Program on Critical Compilation of Physical and Chemical Data coordinated through the Office of Standard Reference Data (OSRD), National Bureau of Standards. Literature searched through 1982. Professor Laughlin is ASM/NBS Data Program Category Editor for binary copper alloys.

The Be-N (Beryllium-Nitrogen) System

9.01218 14.0067

By H.A. Wriedt
Consultant

and

H. Okamoto*
Lawrence Berkeley Laboratory

Equilibrium Diagram

The equilibrium phases of the Be-N system are (1) the liquid, L; (2) the terminal solid solution, (Be), which exists at lower temperatures as cph (αBe) and at higher temperatures as bcc (βBe); (3) the nitride, Be_3N_2, which exists at lower temperatures as cubic αBe_3N_2 and at higher temperatures as hexagonal βBe_3N_2; and (4) the gas, g. An azide, $Be(N_3)_2$, has been reported, which may also be an equilibrium phase of the condensed system. Crystal structure and lattice parameter data are listed in Tables 1 and 2.

No published phase diagram for the Be-N system was found. The three-phase equilibria and special points for the phases are listed in Table 3. The locations of the (Be) solvus, solidus, and liquidus are mostly unknown, as are those of the Be_3N_2 liquidus and the speculative miscibility gap. Because pertinent data are lacking not only for the positions of the univariants and invariants but also for the

*Present address: ASM International, Metals Park, OH 44073.

Table 1 Be-N Crystal Structure Data

Phase	Composition, at.% N	Pearson symbol	Space group	Strukturbericht designation	Prototype	Reference
αBe	~0	*hP2*	$P6_3/mmc$	*A3*	Mg	[King1]
βBe	~0	*cI2*	*Im3m*	*A2*	W	[King2]
αBe_3N_2	~40	*cI80*	*Ia3*	$D5_3$	Anti-Mn_2O_3	[Pearson2]
βBe_3N_2	~40	*hP10*	$P6_3/mmc$	...	βBe_3N_2	[Pearson2]
$Be(N_3)_2$	~86	...	...	...	...	